

Rise and Fall of the Pseudogap in the Emery model: Insights for Cuprates

M. O. Malcolms,^{1,*} Henri Menke,^{1,2} Yi-Ting Tseng,²
Eric Jacob,³ Karsten Held,³ Philipp Hansmann,² and Thomas Schäfer^{1,†}

¹Max-Planck-Institut für Festkörperforschung, Heisenbergstraße 1, 70569 Stuttgart, Germany

²Department of Physics, University of Erlangen-Nürnberg, 91058 Erlangen, Germany

³Institute of Solid State Physics, TU Wien, 1040 Vienna, Austria

The pseudogap in high-temperature superconducting cuprates is an exotic state of matter, displaying emerging Fermi arcs and a momentum-selective suppression of states upon cooling. We show how these phenomena are originating in the three-band Emery model by performing cutting-edge dynamical vertex approximation calculations for its normal state. For the hole-doped parent compound our results demonstrate the formation of a pseudogap due to short-ranged commensurate antiferromagnetic fluctuations. At larger doping values, progressively, incommensurate correlations and a metallic regime appear. Our results are in qualitative agreement with the normal state of cuprates, and, hence, represent a crucial step towards the uniform description of their phase diagrams within a single theoretical framework.

Introduction. The intriguing properties of layered cuprate superconductors have not lost their fascination since their discovery in 1986 by Bednorz and Müller [1]. The reason for the unbroken interest is at least three-fold: First, their temperature/doping phase diagram is unusually rich [2], exhibiting quantum magnetism, unconventional superconductivity, strange metallicity and the famous pseudogap regime, as a function of temperature and (hole-)doping. Second, cuprates hold the potential for immensely impactful technological applications. Third, the physical mechanisms behind this rich phenomenology are –after almost 40 years of intense community effort– still highly debated. The reason for the latter is deeply rooted in the fact that cuprates are strongly interacting quantum many-body systems, whose properties cannot be explained by a simple single-particle picture: their electrons are strongly correlated in space and in time.

Adding to the complexity of this material class, it has been realized early on that, due to the close vicinity of the oxygen p -orbitals to the Fermi level, the oxygen p_x/y -orbitals of the CuO_2 two-dimensional layers are relevant besides the copper $d_{x^2-y^2}$ -orbitals; and that the undoped parent compounds are charge-transfer, rather than (single-orbital) Mott-Hubbard insulators [3]. In order to explicitly include charge-transfer processes the minimal model thus has to treat the oxygen p - on top of the copper d -orbitals, enabling, among other properties, (Zhang-Rice) singlet-formation between these orbitals [4]. These considerations led to the famous three-band model proposed by Emery [5], Varma, Schmitt-Rinks, and Abrahams [6] and later refined by Andersen and coworkers [7]. In this respect, the situation in cuprates is largely differing from the case of the recently discovered infinite-layer nickelate superconductors [8]. For the latter case first-principle-based calculations indicate that indeed a single-band Hubbard model could suffice for the low-energy description of superconductivity and putative pseudogap [9, 10]; for recent reviews on the single-band Hubbard

model see [11, 12].

One of the hallmark features of the normal state of the cuprates is the so-called pseudogap, a suppression of the spectral function near the antinode $(\pi, 0)$ at low hole-doping levels. This intriguing regime, which shows no signs of a thermodynamic phase transition, can be detected experimentally, for example, by nuclear magnetic resonance (NMR) Knight shift [13], or, even more directly, by angle-resolved photoemission spectroscopy (ARPES) [14–20].

A reliable modeling of cuprates, not only has to take into account their multi-orbital nature, but should also

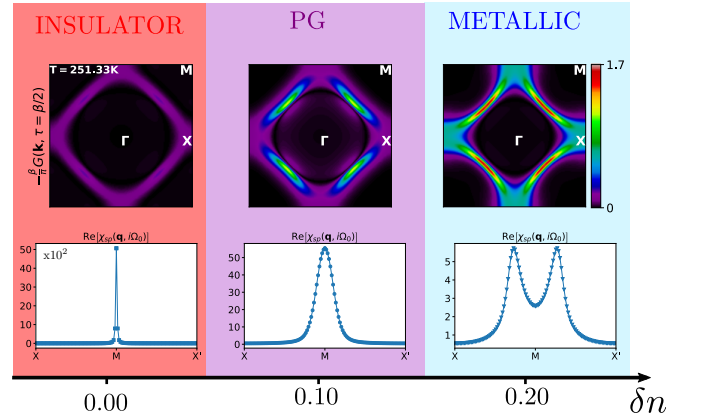


FIG. 1. Sketch of the phase diagram of the normal phase regime of the three-orbital Emery model for cuprates, for a fixed temperature $T = 251.33$ K as a function of hole doping, as actually calculated by the dynamical vertex approximation. After an insulating regime the pseudogap (PG) first rises and then falls off again with the system eventually becoming a conventional metal. In the PG regime, the Fermi surface is reduced to Fermi arcs (upper row). Concomitantly, commensurate antiferromagnetic and incommensurate magnetic fluctuations are present, demonstrated by the momentum-dependent magnetic susceptibility (lower row). The shadings serve as a guide to the eye throughout the manuscript.

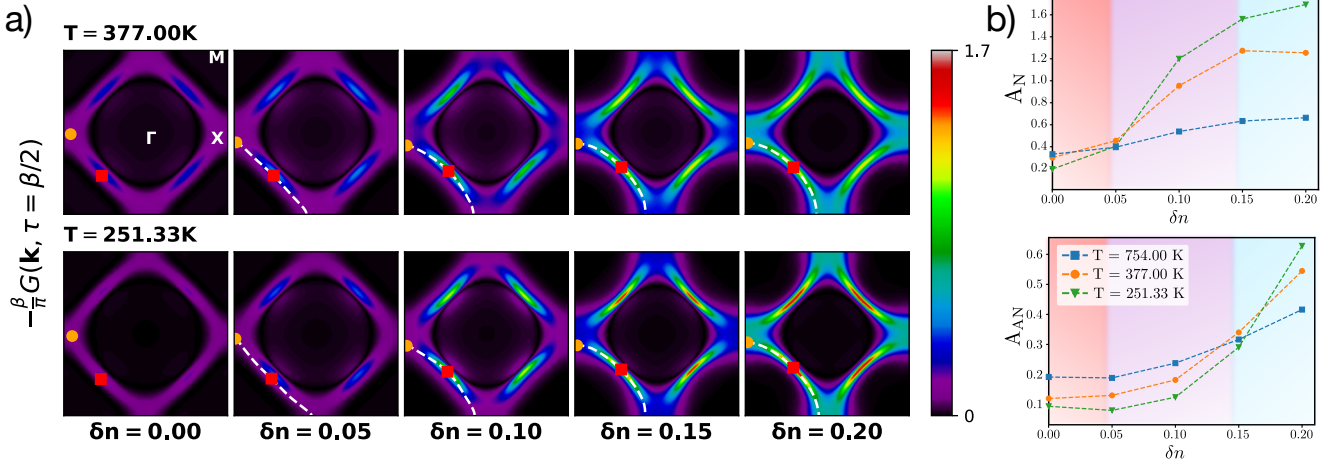


FIG. 2. (a) Hole-doping evolution of DGA \mathbf{k} -resolved spectral intensities at the Fermi energy for $T = t_{pp}/20 = 377\text{ K}$ (upper panels) and $T = t_{pp}/30 = 251.33\text{ K}$ (lower panels) with displayed interacting Fermi plus Luttinger surface (dashed white line) and the position of the nodal (red square) and anti-nodal (orange circle) points. (b) Hole-doping and temperature dependence of the spectral function at the interacting Fermi surface at the nodal (upper panel) and anti-nodal (lower panel) points. The shaded background highlights the different crossovers revealed by DGA, indicated in Fig. 1 by the same color.

be able to reveal the crossover into the pseudogap regime upon hole doping. While the pseudogap in the Hubbard model has been firmly established by numerous approaches [21–25], the presence and nature of the pseudogap in the hole-doped Emery model has been, to the best of our knowledge, not thoroughly investigated yet: Despite efforts with a variety of techniques [26–31] and calculations for the superconducting properties [32–34], the evolution of the Fermi surface and the precise nature of the spin fluctuations, essential hallmarks of the pseudogap regime, have not been reported before.

In this Letter we now make significant progress in the universal description of the cuprates' phase diagrams by extending the state-of-the-art λ -corrected dynamical vertex approximation (DGA) to the three-band Emery model [35, 36]. With our extension to three bands we establish the normal phase regime of the Emery model in two dimensions with realistic cuprate parameters as a function of temperature and hole doping. We document the fate of the pseudogap from its rise out of the insulating parent compound to its eventual fall in the metallic regime (see Fig. 1). We further discuss the relevance of our calculations for spectroscopic experiments, a crucial step on the way to a comprehensive theoretical description of the cuprates.

Model and Method. We consider the three-band Emery model that accounts for the copper-oxygen hybridized character of the single band that crosses the Fermi surface (see Supplemental Materials [35]) and whose Hamiltonian reads

$$H = \sum_{\mathbf{k}, \sigma} \psi_{\mathbf{k}, \sigma}^\dagger \bar{h}_0(\mathbf{k}) \psi_{\mathbf{k}, \sigma} + U \sum_i n_{i, \uparrow}^d n_{i, \downarrow}^d, \quad (1)$$

where $\psi_{\mathbf{k}, \sigma}^\dagger = (d_{\mathbf{k}, \sigma}^\dagger, p_{x, \mathbf{k}, \sigma}^\dagger, p_{y, \mathbf{k}, \sigma}^\dagger)$ contains the electronic creation operators on the copper $d_{x^2-y^2}$ - and the oxygen p_x - and p_y -orbitals with spin σ and momentum \mathbf{k} . U quantifies the local part of the Coulomb repulsion restricted to the copper $d_{x^2-y^2}$ -orbital and $n_{i, \sigma}^d = d_{i, \sigma}^\dagger d_{i, \sigma}$ is the number operator per spin for the d -orbital. On the square lattice, setting the distance between unit cells to unity, the non-interacting Hamiltonian $\bar{h}_0(\mathbf{k})$ in Eq. (1) reads

$$\bar{h}_0(\mathbf{k}) = \begin{pmatrix} \epsilon_d & t_{pd}s_{k_x} & t_{pd}s_{k_y} \\ t_{pd}s_{k_x}^* & \epsilon_p + t'_{pp}\epsilon_{k_x} & t_{pp}s_{k_x}^*s_{k_y} \\ t_{pd}s_{k_y}^* & t_{pp}s_{k_y}^*s_{k_x} & \epsilon_p + t'_{pp}\epsilon_{k_y} \end{pmatrix}, \quad (2)$$

with $\epsilon_k = 2 \cos k$ and $s_k = 2ie^{i\frac{k}{2}} \sin \frac{k}{2}$. The on-site energies on the Cu and O orbitals are denoted ϵ_d and ϵ_p , respectively. The nearest-neighbor Cu-O hopping is denoted by t_{pd} , while t_{pp} and t'_{pp} denote the direct nearest-neighbor O-O hopping and the indirect one through the Cu site, respectively.

In our calculations, following Refs. [32, 37], we adopt $t_{pp} \sim 650\text{ meV}$, $\epsilon_p = 2.3t_{pp} = 1.5\text{ eV}$, $t_{pd} = 2.1t_{pp} = 1.37\text{ eV}$ and $t'_{pp} = 0.2t_{pp} = 130\text{ meV}$ for the non-interacting system in Eq. (2); ϵ_p has been obtained by subtracting the same double-counting contribution as in Ref. [37]. Motivated by X-ray photoemission spectroscopy (XPES) experiments [38, 39], in this work, we fix the interaction value to $U = 10t_{pp} = 6.5\text{ eV}$, while the total electronic density $n = n_{d_{x^2-y^2}} + n_{p_x} + n_{p_y}$ and the temperature T are varied.

We analyze the normal state of the model by means of ladder DGA [41], a diagrammatic extension [42] of the dynamical mean-field theory [43] which is particularly suited for treating spatial and temporal correlations.

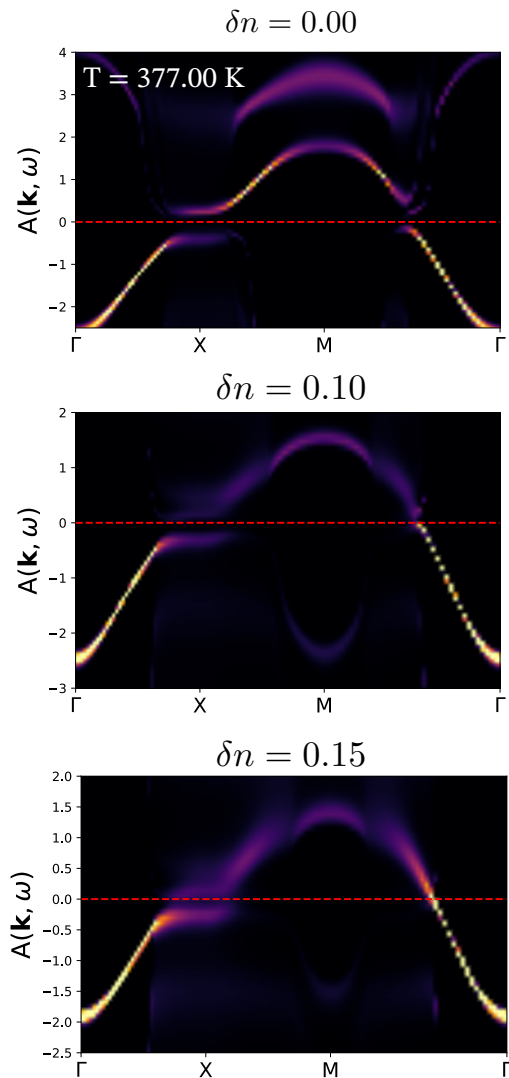


FIG. 3. Hole-doping evolution of ladder DGA spectral intensities along the high-symmetry path $\Gamma X M \Gamma$ of the Brillouin zone for $T = 377$ K obtained by MaxEnt analytical continuation [40]. The dashed red line denotes the Fermi level of the interacting system. The intensity grows from purple to yellow.

Specific properties of this method are its arbitrarily fine momentum resolution and applicability in the strong-coupling regime, both of which being (i) highly desired for the description of the pseudogap regime and (ii) advantages over cluster (see, e.g., [27, 28, 32–34, 44, 45]) or other diagrammatic (see, e.g., [30]) techniques, respectively. As such, DGA has already been very successful for single-band systems over the past years [9, 22, 42]. We now extend this method to the Emery model [35].

Fermiology: Fermi surfaces and arcs. We first investigate the hole-doping and temperature evolution of the electronic spectrum. Fig. 2(a) displays the momentum dependence of the Green function in imag-

inary time $\tau = \beta/2$ ($\beta = 1/T$) for different temperatures: $T = 377$ K, 251.33 K and various values of hole-doping: $\delta n = 0.00, 0.05, 0.10, 0.15, 0.20$ with $\delta n = 5 - n$. It is directly related to the spectrum in an energy interval $\sim T$ around the Fermi energy, $-\frac{\beta}{\pi} G(\mathbf{k}, \tau = \beta/2) = \frac{\beta}{2\pi} \int d\omega \frac{A(\mathbf{k}, \omega)}{\cosh(\beta\omega/2)}$, and avoids the perils of the ill-conditioned analytical continuation.

Fig. 2(a) also displays the correlated Fermi plus Luttinger surface, indicated as dashed white lines and determined as $\text{Re } G(\mathbf{k}_{\text{FS}}, i\omega_n \rightarrow 0) = 0$, where $i\omega_n \rightarrow 0$ is obtained as a linear extrapolation of the two first fermionic Matsubara frequencies. The minima (maxima) of $-\frac{\beta}{\pi} G(\mathbf{k}_{\text{FS}}, \tau = \beta/2)$ on the correlated Fermi surface defines the anti-nodal (nodal) point indicated by the orange (red) dot (square) in Fig. 2(a). For both temperatures, $T = 377$ K and 251.33 K, the electronic spectrum evolves upon doping from an insulating parent compound (undoped system, $\delta n = 0.00$) characterized by a very low spectral intensity over the Fermi surface into a metallic regime ($\delta n = 0.20$). In between, a pseudogap phase, marked by the appearance of a Fermi arc structure at the Fermi level, emerges ($\delta n = 0.10$), which is a hallmark feature of cuprates [16]. Upon cooling, the spectrum intensity over the Fermi surface reduces for the undoped system while it increases for the highest doping analyzed here ($\delta n = 0.20$), which documents the evolution of the system from an insulating into a metallic state upon hole-doping. In addition, from $\delta n = 0.05$ to $\delta n = 0.10$ in Fig. 2(a), for both temperatures $T = 377$ K and 251.33 K, the reduction in the scattering processes between the quasiparticles leads to a topological reconstruction of the Fermi surface from a electron-like to an hole-like shape (Lifshitz transition) [46, 47]. For $\delta n = 0.00$ (insulating state) no Fermi surface can be defined, since the system is completely gapped.

In Fig. 2(a) we further observe that even deep inside the metallic state ($\delta n = 0.20$), non-local correlation effects alter the Fermi surface (see [35] for a comparison with DMFT). These changes of the Fermi surface arise from the momentum dependence of the real part of the electronic self-energy ($\text{Re } \Sigma_{\mathbf{k}, i\omega_n}$) and are minor compared to the much more dramatic opening of the pseudogap at the antinode. This pseudogap opening instead is due to the momentum dependence of $\text{Im} \Sigma_{\mathbf{k}, i\omega_n}$ and can severely affect the superconducting instabilities as previously shown [48].

Fig. 2(b) shows the doping evolution of the nodal (upper panel) and anti-nodal (lower panel) spectral weight for different temperatures. For the undoped system we observe that upon cooling the spectral weight at both node and anti-node decreases, corroborating the notion of an insulating regime. However, at $\delta n = 0.05$, while the spectral function at the antinodal point still decreases upon cooling, it saturates at the nodal one. Such behavior indicates a crossover into the pseudogap phase since

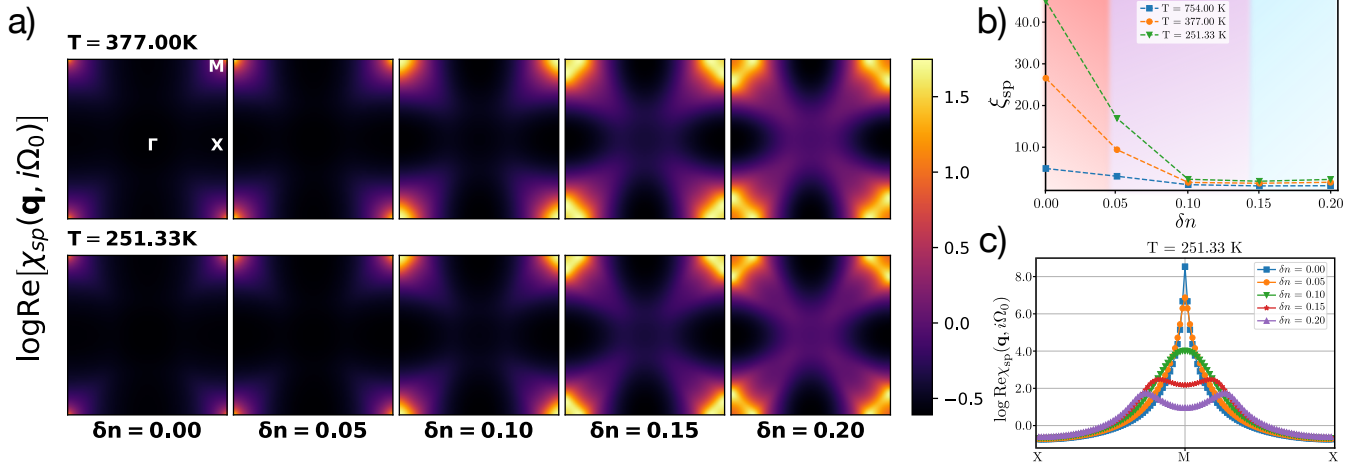


FIG. 4. (a) Hole-doping evolution of the logarithm of the \mathbf{q} -resolved ladder DGA static spin susceptibility for $T = 377$ K (upper panels) and $T = 251.33$ K (lower panels). (b) Hole-doping and temperature dependence of ladder DGA spin correlation length. (c) Hole-doping evolution of the logarithm of the ladder DGA static spin susceptibility along the high symmetry path XMX of the Brillouin zone for $T = 251.33$ K.

at a higher doping $\delta n = 0.10$ the spectral function at the nodal point shows the inverse behavior of the antinodal one. That is, it increases now upon decreasing temperature indicating the metallicity of the nodal point. With further doping to $\delta n = 0.15$, a saturation at the antinodal point is also observed. This point introduces a second crossover into a metallic phase for all momenta that can be observed at $\delta n = 0.20$, where both spectral weights at node and antinode increase when cooling the system, the characteristic feature of a metal.

In order to investigate further the crossovers observed from the Green function on the Matsubara axis, we present in Fig. 3 the energy-momentum dispersion of the spectrum around the Fermi level. Here we plot the spectral function at real (instead of Matsubara) frequencies, obtained by MaxEnt analytical continuation [40] at $T = 377$ K for relevant dopings along the $\Gamma X M \Gamma$ high-symmetry path of the Brillouin zone. This high-symmetry path includes both the nodal and antinodal points. The undoped system ($\delta n = 0.00$) clearly shows an insulating behavior marked by the presence of a complete gap (upper panel) at the Fermi level. For $\delta n = 0.10$, at the insulator-to-pseudogap crossover (middle panel), electronic states emerge along the $M\Gamma$ -direction while a gap still persists along the ΓX -direction. Deep inside the pseudogap phase at $\delta n = 0.15$ (lower panel), a few electronic states appear around the Fermi level along the ΓX -direction while such states are more prominent along the $M\Gamma$ -direction, a typical feature of the pseudogap phase.

Magnetic susceptibilities and correlation lengths. An interesting question is whether the pseudogap phase is driven by spin fluctuations, as demonstrated for the single-band Hubbard model by fluctuation diagnostics techniques [49–51]. Fig. 4(b) shows the doping depen-

dence of the magnetic correlation length ξ obtained by an Ornstein-Zernike fit of the static magnetic lattice susceptibility for different temperatures. Note that, as we consider an ideal two-dimensional system, neither the magnetic correlation length nor the static magnetic lattice susceptibility diverge at finite temperatures [35, 52]. For all temperatures in Fig. 4(b), the magnetic correlation length rapidly decreases upon hole-doping, reaching always its maxima in the undoped system ($\delta n = 0.00$). Differently from the undoped system where the insulating phase seems to be driven by long-ranged spin fluctuations characterized by a large correlation length (~ 45 sites at $T = 251.33$ K), deep inside the pseudogap phase ($\delta n = 0.10$) the magnetic correlation is rather small ($\lesssim 5$ lattice sites at $T = 251.33$ K) and only slightly varying with temperature and doping. This indicates that the pseudogap regime in the Emery model is driven by short-ranged dynamical spin fluctuations included in the ladder DGA construction of the electronic self-energy [35].

To extend our analysis, Fig. 4(a) displays the doping and temperature dependence of the static magnetic lattice susceptibility over the Brillouin zone. For all the temperatures, at low hole-doping ($\delta n < 0.15$) where the system is either insulating or in the pseudogap regime, the antiferromagnetic correlations are commensurately peaked at $\mathbf{q} = \mathbf{M} = (\pi, \pi)$, while inside the metallic phase ($\delta n \geq 0.15$) they become incommensurate and peak at $\mathbf{q} = (\pi, \pi \pm \delta)$, $(\pi \pm \delta, \pi)$. The same feature is observed in Fig. 4(c) where the static magnetic lattice susceptibility is shown along the XMX high-symmetry path of the Brillouin zone as a function of doping at $T = 251.33$ K.

Discussion and relation to experiments. We now compare our results with experimental studies for one of

the most prominent members of the cuprate family: $\text{La}_{2-x}\text{Sr}_x\text{CuO}_4$ (LSCO). The model parameters used for our calculations fit reasonably well with the parameters determined for LSCO previously by ab-initio methods [37], except for ε_p , which is slightly smaller in our study. For LSCO a large number of experimental studies that connect to our Emery model calculation in the paramagnetic phase exist: the evolution of the Fermi surface, the nature of the magnetic fluctuations, and the magnetic correlation length have been measured as a function of Sr-doping, corresponding to hole-doping in our calculations.

Let us now compare experiment to theory: For the lowest temperatures that we analyzed, we find the pseudogap regime in a doping range of $\delta n \in [0.05, 0.15]$. This is in good agreement with ARPES [53] and Nernst effect [54] measurements performed at $T \approx 100$ K. The underlying Fermi surface determined by ARPES [16] evolves similarly to our calculations: at small dopings the spectral weight is low and concentrated around the node, while the Fermi arcs enlarge at intermediate doping, before the Fermi surface eventually closes at $\delta n \approx 0.2$, indicating the rise and fall of the pseudogap.

Regarding magnetism, a crossover from commensurate to incommensurate magnetic fluctuations has been observed in inelastic neutron scattering experiments for LSCO [55, 56]. There, the onset of incommensurability has been determined to start already at very small doping levels, with a direct proportionality of incommensurability and doping $\delta \propto \delta n$ [56]. Our computational results have a non-zero doping threshold for incommensurate fluctuations instead, which we attribute to the lower temperatures $T \lesssim 40$ K, at which the experiments have been performed. Let us note that incommensurability has also been measured in $\text{YBa}_2\text{Cu}_3\text{O}_{6+x}$ [57], however it seems to be absent in $\text{HgBa}_2\text{CuO}_{4+\delta}$ [58].

The (in-plane) magnetic correlation length ξ has been shown to significantly drop from about 15 lattice spacings in LSCO near the parent compound, to about 3-4 lattice spacings in $\delta n \in [0.05, 0.15]$ [59], being in very good agreement with our calculations in the pseudogap regime.

Conclusions and outlook. With cutting-edge DFT calculations we have demonstrated that the Emery model captures the rise and fall of the pseudogap through a series of crossovers from the insulating to the pseudogap to the metallic regime. Our results are in good agreement with the signatures of the normal phase observed in spectroscopic experiments for cuprates. Both the insulating and pseudogap phases are accompanied by (short-range) commensurate antiferromagnetic correlations while the metallic state is dominated by incommensurate ones. Establishing these key features for the normal phase of the fundamental model for cuprates, the three-band Emery model, represents a significant step towards the universal theoretical description of cuprates.

Acknowledgements. We acknowledge fruitful discussions with Nils Wentzell and Paul Worm on the theoretical and numerical part of our work, as well as with Eva Benckiser and Matthias Hepting on experiments on cuprates and critical reading of our manuscript. The work has been supported in part by the Austrian Science Funds (FWF) through Grant DOI 10.55776/Grant DOI 10.55776/I5398 and Grant DOI 10.55776/I5868. We further acknowledge funding by the Austrian Science Funds (FWF) through projects I 5398 F86), I 5868). The authors gratefully acknowledge the scientific support and HPC resources provided by the Erlangen National High Performance Computing Center (NHR@FAU) of the Friedrich-Alexander-Universität Erlangen-Nürnberg (FAU) [hardware funded by the German Research Foundation - DFG], and the computing service facility of the MPI-FKF, responsible for the Bordeaux cluster.

* m.deoliveira@fkf.mpg.de

† t.schaefer@fkf.mpg.de

- [1] J. G. Bednorz and K. A. Müller, Possible high T_c superconductivity in the Ba-La-Cu-O system, *Zeitschrift für Physik B Condensed Matter* **64**, 189 (1986).
- [2] B. Keimer, S. A. Kivelson, M. R. Norman, S. Uchida, and J. Zaanen, From quantum matter to high-temperature superconductivity in copper oxides, *Nature* **518**, 179 (2015).
- [3] J. Zaanen, G. A. Sawatzky, and J. W. Allen, Band gaps and electronic structure of transition-metal compounds, *Phys. Rev. Lett.* **55**, 418 (1985).
- [4] F. C. Zhang and T. M. Rice, Effective Hamiltonian for the superconducting Cu oxides, *Phys. Rev. B* **37**, 3759 (1988).
- [5] V. J. Emery, Theory of high- T_c superconductivity in oxides, *Phys. Rev. Lett.* **58**, 2794 (1987).
- [6] C. Varma, S. Schmitt-Rink, and E. Abrahams, Charge transfer excitations and superconductivity in “ionic” metals, *Solid State Communications* **62**, 681 (1987).
- [7] O. Andersen, A. Liechtenstein, O. Jepsen, and F. Paulsen, LDA energy bands, low-energy Hamiltonians, t' , t'' , $t_{\perp}(k)$, and J_{\perp} , *Journal of Physics and Chemistry of Solids* **56**, 1573 (1995), proceedings of the Conference on Spectroscopies in Novel Superconductors.
- [8] D. Li, K. Lee, B. Y. Wang, M. Osada, S. Crossley, H. R. Lee, Y. Cui, Y. Hikita, and H. Y. Hwang, Superconductivity in an infinite-layer nickelate, *Nature* **572**, 624 (2019).
- [9] M. Kitatani, L. Si, O. Janson, R. Arita, Z. Zhong, and K. Held, Nickelate superconductors—a renaissance of the one-band Hubbard model, *npj Quantum Materials* **5**, 10.1038/s41535-020-00260-y (2020).
- [10] M. Klett, P. Hansmann, and T. Schäfer, Magnetic properties and pseudogap formation in infinite-layer nickelates: Insights from the single-band hubbard model, *Frontiers in Physics* **10**, 834682 (2022).
- [11] M. Qin, T. Schäfer, S. Andergassen, P. Corboz, and E. Gull, The Hubbard Model: A Computational Perspective, *Annual Review of Condensed Matter Physics*

- 13**, 275 (2022), <https://doi.org/10.1146/annurev-conmatphys-090921-033948>.
- [12] D. P. Arovas, E. Berg, S. A. Kivelson, and S. Raghu, The Hubbard Model, *Annual Review of Condensed Matter Physics* **13**, [10.1146/annurev-conmatphys-031620-102024](https://doi.org/10.1146/annurev-conmatphys-031620-102024) (2022), <https://doi.org/10.1146/annurev-conmatphys-031620-102024>.
- [13] H. Alloul, T. Ohno, and P. Mendels, ^{89}Y NMR evidence for a fermi-liquid behavior in $\text{YBa}_2\text{Cu}_3\text{O}_{6+x}$, *Phys. Rev. Lett.* **63**, 1700 (1989).
- [14] A. Damascelli, Z. Hussain, and Z.-X. Shen, Angle-resolved photoemission studies of the cuprate superconductors, *Rev. Mod. Phys.* **75**, 473 (2003).
- [15] A. Kanigel, M. R. Norman, M. Randeria, U. Chatterjee, S. Souma, A. Kaminski, H. M. Fretwell, S. Rosenkranz, M. Shi, T. Sato, T. Takahashi, Z. Z. Li, H. Raffy, K. Kad-owaki, D. Hinks, L. Ozyuzer, and J. C. Campuzano, Evolution of the pseudogap from Fermi arcs to the nodal liquid, *Nature Physics* **2**, 447 (2006).
- [16] T. Yoshida, X. J. Zhou, K. Tanaka, W. L. Yang, Z. Hussain, Z.-X. Shen, A. Fujimori, S. Sahrakorpi, M. Lindroos, R. S. Markiewicz, A. Bansil, S. Komiyama, Y. Ando, H. Eisaki, T. Kakeshita, and S. Uchida, Systematic doping evolution of the underlying Fermi surface of $\text{La}_{2-x}\text{Sr}_x\text{CuO}_4$, *Phys. Rev. B* **74**, 224510 (2006).
- [17] K. M. Shen, F. Ronning, D. H. Lu, F. Baumberger, N. J. C. Ingle, W. S. Lee, W. Meevasana, Y. Kohsaka, M. Azuma, M. Takano, H. Takagi, and Z.-X. Shen, Nodal Quasiparticles and Antinodal Charge Ordering in $\text{Ca}_{2-x}\text{Na}_x\text{CuO}_2\text{Cl}_2$, *Science* **307**, 901 (2005).
- [18] L. Taillefer, Scattering and Pairing in Cuprate Superconductors, *Annual Review of Condensed Matter Physics* **1**, 51 (2010).
- [19] F. Boschini, M. Zonno, E. Razzoli, R. P. Day, M. Michiardi, B. Zwartsenberg, P. Nigge, M. Schneider, E. H. da Silva Neto, A. Erb, S. Zhdanovich, A. K. Mills, G. Levy, C. Giannetti, D. J. Jones, and A. Damascelli, Emergence of pseudogap from short-range spin-correlations in electron-doped cuprates, *npj Quantum Materials* **5**, 6 (2020).
- [20] F. Boschini, M. Zonno, and A. Damascelli, Time-resolved ARPES studies of quantum materials, *Rev. Mod. Phys.* **96**, 015003 (2024).
- [21] B. Kyung, V. Hankevych, A.-M. Daré, and A.-M. S. Tremblay, Pseudogap and Spin Fluctuations in the Normal State of the Electron-Doped Cuprates, *Phys. Rev. Lett.* **93**, 147004 (2004).
- [22] T. Schäfer, N. Wentzell, F. Šimkovic, Y.-Y. He, C. Hille, M. Klett, C. J. Eckhardt, B. Arzhang, V. Harkov, F. Le Régent, A. Kirsch, Y. Wang, A. J. Kim, E. Kozik, E. A. Stepanov, A. Kauch, S. Andergassen, P. Hansmann, D. Rohe, Y. M. Vilks, J. P. F. LeBlanc, S. Zhang, A.-M. S. Tremblay, M. Ferrero, O. Parcollet, and A. Georges, Tracking the Footprints of Spin Fluctuations: A MultiMethod, MultiMessenger Study of the Two-Dimensional Hubbard Model, *Phys. Rev. X* **11**, 011058 (2021).
- [23] F. Krien, P. Worm, P. Chalupa-Gantner, A. Toschi, and K. Held, Explaining the pseudogap through damping and antidamping on the Fermi surface by imaginary spin scattering, *Communications Physics* **5**, 336 (2022).
- [24] Y. M. Vilks, C. Lahaie, and A.-M. S. Tremblay, Antiferromagnetic pseudogap in the two-dimensional Hubbard model deep in the renormalized classical regime, *Physical Review B* **110**, [10.1103/physrevb.110.125154](https://doi.org/10.1103/physrevb.110.125154) (2024).
- [25] F. Šimkovic, R. Rossi, A. Georges, and M. Ferrero, Origin and fate of the pseudogap in the doped Hubbard model, *Science* **385**, eade9194 (2024).
- [26] A. Avella, F. Mancini, F. P. Mancini, and E. Plekhanov, Emery vs. Hubbard model for cuprate superconductors: a composite operator method study, *The European Physical Journal B* **86**, [10.1140/epjb/e2013-40115-3](https://doi.org/10.1140/epjb/e2013-40115-3) (2013).
- [27] L. Fratino, P. Sémon, G. Sordi, and A.-M. S. Tremblay, Pseudogap and superconductivity in two-dimensional doped charge-transfer insulators, *Phys. Rev. B* **93**, 245147 (2016).
- [28] S. S. Dash and D. Sénéchal, Pseudogap transition within the superconducting phase in the three-band Hubbard model, *Physical Review B* **100** (2019).
- [29] T. Mao and M. Jiang, Non-Fermi liquid behavior of scattering rate in three-orbital Emery model (2024), [arXiv:2403.11218](https://arxiv.org/abs/2403.11218) [cond-mat.str-el].
- [30] C. Gauvin-Ndiaye, J. Leblanc, S. Marin, N. Martin, D. Lessnich, and A.-M. S. Tremblay, Two-particle self-consistent approach for multiorbital models: Application to the Emery model, *Phys. Rev. B* **109**, 165111 (2024).
- [31] G. Sordi, G. L. Reaney, N. Kowalski, P. Sémon, and A. M. S. Tremblay, Ambipolar doping of a charge-transfer insulator in the Emery model (2024), [arXiv:2407.19545](https://arxiv.org/abs/2407.19545) [cond-mat.str-el].
- [32] N. Kowalski, S. S. Dash, P. Sémon, D. Sénéchal, and A.-M. Tremblay, Oxygen hole content, charge-transfer gap, covalency, and cuprate superconductivity, *Proceedings of the National Academy of Sciences* **118**, e2106476118 (2021).
- [33] P. Mai, G. Balduzzi, S. Johnston, and T. A. Maier, Orbital structure of the effective pairing interaction in the high-temperature superconducting cuprates, *npj Quantum Materials* **6**, 26 (2021).
- [34] P. Mai, G. Balduzzi, S. Johnston, and T. A. Maier, Pairing correlations in the cuprates: A numerical study of the three-band Hubbard model, *Phys. Rev. B* **103**, 144514 (2021).
- [35] See Supplemental Material available at
- [36] A. Galler, P. Thunström, P. Gunacker, J. M. Tomczak, and K. Held, Ab initio dynamical vertex approximation, *Phys. Rev. B* **95**, 115107 (2017).
- [37] C. Weber, C. Yee, K. Haule, and G. Kotliar, Scaling of the transition temperature of hole-doped cuprate superconductors with the charge-transfer energy, *Europhysics Letters* **100**, 37001 (2012).
- [38] A. E. Bocquet, T. Mizokawa, T. Saitoh, H. Namatame, and A. Fujimori, Electronic structure of 3d-transition-metal compounds by analysis of the 2p core-level photoemission spectra, *Phys. Rev. B* **46**, 3771 (1992).
- [39] A. E. Bocquet, T. Mizokawa, K. Morikawa, A. Fujimori, S. R. Barman, K. Maiti, D. D. Sarma, Y. Tokura, and M. Onoda, Electronic structure of early 3d-transition-metal oxides by analysis of the 2p core-level photoemission spectra, *Phys. Rev. B* **53**, 1161 (1996).
- [40] A. Reymbaut, A.-M. Gagnon, D. Bergeron, and A.-M. S. Tremblay, Maximum entropy analytic continuation for frequency-dependent transport coefficients with nonpositive spectral weight, *Phys. Rev. B* **95**, 121104 (2017).
- [41] A. Toschi, A. A. Katanin, and K. Held, Dynamical vertex approximation; A step beyond dynamical mean-field theory, *Phys. Rev. B* **75**, 045118 (2007).
- [42] G. Rohringer, H. Hafermann, A. Toschi, A. A. Katanin,

- A. E. Antipov, M. I. Katsnelson, A. I. Lichtenstein, A. N. Rubtsov, and K. Held, Diagrammatic routes to nonlocal correlations beyond dynamical mean field theory, *Rev. Mod. Phys.* **90**, 025003 (2018).
- [43] A. Georges, G. Kotliar, W. Krauth, and M. J. Rozenberg, Dynamical mean-field theory of strongly correlated fermion systems and the limit of infinite dimensions, *Rev. Mod. Phys.* **68**, 13 (1996).
- [44] T. Maier, M. Jarrell, T. Pruschke, and M. H. Hettler, Quantum cluster theories, *Rev. Mod. Phys.* **77**, 1027 (2005).
- [45] P. Mai, B. Cohen-Stead, T. A. Maier, and S. Johnston, Fluctuating charge-density-wave correlations in the three-band Hubbard model (2024), [arXiv:2405.13164](https://arxiv.org/abs/2405.13164) [[cond-mat.str-el](https://arxiv.org/abs/2405.13164)].
- [46] W. Wu, M. S. Scheurer, S. Chatterjee, S. Sachdev, A. Georges, and M. Ferrero, Pseudogap and Fermi-Surface Topology in the Two-Dimensional Hubbard Model, *Phys. Rev. X* **8**, 021048 (2018).
- [47] M. Meixner, H. Menke, M. Klett, S. Heinzlmann, S. Andergassen, P. Hansmann, and T. Schäfer, Mott transition and pseudogap of the square-lattice Hubbard model: Results from center-focused cellular dynamical mean-field theory, *SciPost Phys.* **16**, 059 (2024).
- [48] M. Kitatani, L. Si, P. Worm, J. M. Tomczak, R. Arita, and K. Held, Optimizing superconductivity: From cuprates via nickelates to palladates, *Phys. Rev. Lett.* **130**, 166002 (2023).
- [49] O. Gunnarsson, T. Schäfer, J. P. F. LeBlanc, E. Gull, J. Merino, G. Sangiovanni, G. Rohringer, and A. Toschi, Fluctuation Diagnostics of the Electron Self-Energy: Origin of the Pseudogap Physics, *Phys. Rev. Lett.* **114**, 236402 (2015).
- [50] W. Wu, M. Ferrero, A. Georges, and E. Kozik, Controlling Feynman diagrammatic expansions: Physical nature of the pseudogap in the two-dimensional Hubbard model, *Phys. Rev. B* **96**, 041105(R) (2017).
- [51] T. Schäfer and A. Toschi, How to read between the lines of electronic spectra: the diagnostics of fluctuations in strongly correlated electron systems, *Journal of Physics: Condensed Matter* **33**, 214001 (2021).
- [52] N. D. Mermin and H. Wagner, Absence of Ferromagnetism or Antiferromagnetism in One- or Two-Dimensional Isotropic Heisenberg Models, *Phys. Rev. Lett.* **17**, 1307 (1966).
- [53] T. Yoshida, M. Hashimoto, S. Ijeta, A. Fujimori, K. Tanaka, N. Mannella, Z. Hussain, Z.-X. Shen, M. Kubota, K. Ono, S. Komiya, Y. Ando, H. Eisaki, and S. Uchida, Universal versus Material-Dependent Two-Gap Behaviors of the High- T_c Cuprate Superconductors: Angle-Resolved Photoemission Study of $\text{La}_{2-x}\text{Sr}_x\text{CuO}_4$, *Phys. Rev. Lett.* **103**, 037004 (2009).
- [54] O. Cyr-Choinière, R. Daou, F. Laliberté, C. Collignon, S. Badoux, D. LeBoeuf, J. Chang, B. J. Ramshaw, D. A. Bonn, W. N. Hardy, R. Liang, J.-Q. Yan, J.-G. Cheng, J.-S. Zhou, J. B. Goodenough, S. Pyon, T. Takayama, H. Takagi, N. Doiron-Leyraud, and L. Taillefer, Pseudogap temperature T^* of cuprate superconductors from the Nernst effect, *Phys. Rev. B* **97**, 064502 (2018).
- [55] R. J. Birgeneau, Y. Endoh, K. Kakurai, Y. Hidaka, T. Murakami, M. A. Kastner, T. R. Thurston, G. Shirane, and K. Yamada, Static and dynamic spin fluctuations in superconducting $\text{La}_{2-x}\text{Sr}_x\text{CuO}_4$, *Phys. Rev. B* **39**, 2868 (1989).
- [56] K. Yamada, C. H. Lee, K. Kurahashi, J. Wada, S. Wakimoto, S. Ueki, H. Kimura, Y. Endoh, S. Hosoya, G. Shirane, R. J. Birgeneau, M. Greven, M. A. Kastner, and Y. J. Kim, Doping dependence of the spatially modulated dynamical spin correlations and the superconducting-transition temperature in $\text{La}_{2-x}\text{Sr}_x\text{CuO}_4$, *Phys. Rev. B* **57**, 6165 (1998).
- [57] D. Haug, V. Hinkov, Y. Sidis, P. Bourges, N. B. Christensen, A. Ivanov, T. Keller, C. T. Lin, and B. Keimer, Neutron scattering study of the magnetic phase diagram of underdoped $\text{YBa}_2\text{Cu}_3\text{O}_{6+x}$, *New Journal of Physics* **12**, 105006 (2010).
- [58] Z. W. Anderson, Y. Tang, V. Nagarajan, M. K. Chan, C. J. Dorow, G. Yu, D. L. Abernathy, A. D. Christianson, L. Mangin-Thro, P. Steffens, T. Sterling, D. Reznik, D. Bounoua, Y. Sidis, P. Bourges, and M. Greven, Gapped commensurate antiferromagnetic response in a strongly underdoped model cuprate superconductor (2024), [arXiv:2412.03524](https://arxiv.org/abs/2412.03524) [[cond-mat.supr-con](https://arxiv.org/abs/2412.03524)].
- [59] R. J. Birgeneau, D. R. Gabbe, H. P. Jenssen, M. A. Kastner, P. J. Picone, T. R. Thurston, G. Shirane, Y. Endoh, M. Sato, K. Yamada, Y. Hidaka, M. Oda, Y. Enomoto, M. Suzuki, and T. Murakami, Antiferromagnetic spin correlations in insulating, metallic, and superconducting $\text{La}_{2-x}\text{Sr}_x\text{CuO}_4$, *Phys. Rev. B* **38**, 6614 (1988).